AGU PUBLICATIONS

JGR

Journal of Geophysical Research: Atmospheres

RESEARCH ARTICLE
10.1002/2014JD021542

Key Points:
- Internal variability is simulated in a regional model ensemble
- Seasonal tropical cyclone frequency exhibits large internal variability
- Vertical wind shear is a potentially important contributing factor

Correspondence to:
J. M. Done,
done@ucar.edu

Citation:
Done, J. M., C. L. Bruyère, M. Ge, and A. Jaye (2014), Internal variability of North Atlantic tropical cyclones, *J. Geophys. Res. Atmos.*, *119*, 6506–6519, doi:10.1002/2014JD021542.

Received 7 FEB 2014
Accepted 21 MAY 2014
Accepted article online 26 MAY 2014
Published online 10 JUN 2014

Internal variability of North Atlantic tropical cyclones

James M. Done[1], Cindy L. Bruyère[1,2], Ming Ge[1], and Abigail Jaye[1]

[1]National Center for Atmospheric Research, Boulder, Colorado, USA, [2]Environmental Sciences and Management, North-West University, Potchefstroom, South Africa

Abstract Using a regional model initial condition ensemble, this study quantifies the magnitude of internal variability of North Atlantic tropical cyclone frequency for a case study year and identifies potential physical sources. For tropical cyclone formations from easterly waves, the simulated internal variability of tropical cyclone frequency for 1998 is approximately two fifths of the total (externally forced and internal) variability of observed tropical cyclone frequency. The simulated internal variability of tropical cyclone frequency is found to arise in approximately equal measure from variability of easterly wave occurrence and development and variability of the transition from incipient warm cores to tropical cyclones. Variable interaction between developing tropical cyclones and vertical wind shear associated with upper level cyclones is identified as a potentially important contributing factor to tropical cyclone internal variability.

1. Introduction

Weather and climate variability arises from external forcing, such as greenhouse gases, aerosols, volcanic emissions, and solar variability, and internal processes due to nonlinear relations and multiscale feedbacks within the system. The relative importance of internal variability (IV) for both the real and modeled climate increases with decreasing temporal and spatial scales [*Hawkins and Sutton*, 2009, 2010]. On regional scales, IV can exceed forced variability, where it can become large enough to reverse 50 year externally forced warming trends [*Deser et al*., 2012, 2013].

Limited area domain modeling studies, in which the external forcing is represented at the lateral and lower domain boundaries, have shown IV varies by season [*Caya and Biner*, 2004], geographic location [*Rinke et al*., 2004], domain size [*Vannitsem and Chomé*, 2005; *Alexandru et al*., 2007; *Leduc and Laprise*, 2009], and geophysical variable [*Christensen et al*., 2001]. IV therefore appears to be an intrinsic property of the system and external forcing rather than a property of the initial condition perturbations [*Giorgi and Bi*, 2000; *Lucas-Picher et al*., 2008]. For the case of a large ensemble and long-period global climate model simulations, IV is equivalent to the transient eddy variability, owing to the property of ergodicity (time and ensemble means are equal) [*Nikiéma and Laprise*, 2013]. For the case of limited area models on the other hand, the constraints of the lateral boundary conditions violates the property of ergodicity and together with the additional constraints of parameterizations and numerical diffusion this results in a damped representation of IV in limited area models [e.g., *Christensen et al*., 2001].

It is likely that precipitating convective systems in particular exhibit large IV owing to the multiscale nature of their formation and evolution [e.g., *Christensen et al*., 2001]. Tropical cyclones (TCs) may be an extreme case owing to their development under weak large-scale dynamical forcing of the tropics that allows IV to accumulate. *Villarini and Vecchi* [2012] showed IV to be a higher fraction of total prediction uncertainty for North Atlantic TC frequency than for regional surface temperature across a broad range of timescales. Regional ensemble modeling studies have shown that for TC frequency the magnitude of IV and interannual variability can be comparable (see *Jourdain et al*. [2011] for the Southwest Pacific and *Au-Yeung and Chan* [2012] and *Wu et al*. [2012] for the northwest Pacific). Similar studies using global models suggest lower IV of TC frequency over the North Atlantic than over the northwest Pacific [*Zhao et al*., 2009; *Chen and Lin*, 2011, 2013].

The specific mechanisms for the growth of IV of TC frequency remain largely unknown. Using ensemble simulations, *Nikiéma and Laprise* [2011a, 2011b] noted parallels between the IV of regional climate and the energy conversions taking place in weather systems. They showed rapid increases in IV due to the heating of warm perturbations through interactions of potential temperature variations with diabatic heating

from condensation and convection. *Alexandru et al*. [2007] found large geopotential height IV downstream of strong convective events, and *Diaconescu et al*. [2012] showed growth of IV through baroclinic instability. For TC frequency in particular, convective instability is a likely source of IV. *Jourdain et al*. [2011] suggest that nonlinear interactions of mesoscale convective systems at the TC genesis stage through elastic interaction, straining, and vortex merger can be important for the IV of TC frequency. A recent ensemble study [*Wu et al*., 2012] showed that IV increases during the transition from less organized disturbances to the well-organized coherent TCs.

Using a regional model initial condition ensemble, this study explores the magnitude and physical sources of IV of North Atlantic TC frequency. Following *Nikiéma and Laprise* [2013], IV is defined here as the intermember spread in an ensemble driven by identical lateral and lower boundary conditions representing the external forcing. Specifically, we pose the following questions:

1. What is the contribution of IV to total TC frequency variability?
2. What are the physical sources of IV of TC frequency?

Model setup, ensemble design, and analysis approach are described in section 2. Results are presented in section 3 and discussed in section 4. Conclusions are presented in section 5.

2. Method

An ensemble experiment described here is designed to quantify the magnitude of IV of TC frequency and to provide a data set to explore potential physical sources of IV.

2.1. Regional Model Setup

The atmosphere-only Weather Research and Forecasting (WRF) model [*Skamarock et al*., 2008] version 3.1 is driven by European Centre for Medium-Range Weather Forecasts Re-Analysis Interim data [*Simmons et al*., 2006] for a single year. The year 1998 is chosen because of a high level of observed TC activity including 14 tropical storms, 10 hurricanes, and three major hurricanes and a high proportion of TCs (50%) that developed over the eastern tropical North Atlantic (International Best Track Archive for Climate Stewardship (IBTrACS data)) [*Knapp et al*., 2010]. The intention is to isolate and understand IV of TCs that develop from easterly waves and limit contamination from TCs that follow different genesis pathways and therefore may exhibit different IV characteristics. Model options are selected for long-term simulation including a wide lateral boundary zone [*Giorgi et al*., 1993] with combined linear exponential relaxation following *Liang et al*. [2001], updated lower boundary conditions of observed sea surface temperature (SST), and climatological surface albedo and vegetation fraction. A hydrostatic pressure vertical coordinate is used with 51 levels such that levels are terrain following near the surface transitioning to pressure surfaces near the model top at 10 hPa. The horizontal grid spacing of 36 km is sufficient to capture reasonable TC frequency and track information [*Done et al*., 2013].

Shortwave and longwave radiation is treated using the Community Atmosphere Model version 3 radiation scheme [*Collins et al*., 2006]. Cumulus convection is parameterized using the Kain-Fritsch scheme [*Kain and Fritsch*, 1990], including a parameterization of shallow convection. Explicit precipitation processes are parameterized by the WRF single-moment six-class microphysics [*Hong and Lim*, 2006]. Boundary layer and surface processes are represented by the nonlocal Yonsei University (YSU) boundary layer scheme [*Hong and Pan*, 1996] and the Noah land surface model [*Chen and Dudhia*, 2001] with four soil layers.

A key component of the experimental design is a large domain (13,644 km × 8388 km or 379 × 233 grid points, shown in Figure 1) to ensure full spin-up of small scales and to minimize constraints on IV by the domain boundaries [*Laprise et al*., 2012]. Interior domain nudging is not applied to further minimize system constraints. *Crétat et al*. [2011] showed that the genesis and development of rain-bearing systems that are reproducible were associated with larger scale features than the regional model domain size, whereas the morphological features such as location and intensity remain highly variable. Since TC genesis is a multiscale process, many important processes occur on scales smaller than the domain size thereby permitting substantial IV within our domain. The eastern boundary is located such that each ensemble member has identical easterly wave activity entering the domain and restricts contributions to IV to those processes operating within the domain. However, this also means that TC genesis in the eastern North

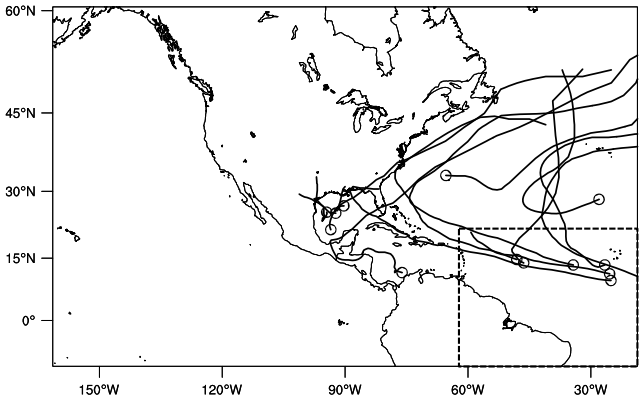

Figure 1. Model domain and terrain height (m). Tracks of observed tropical cyclones for 1998 are indicated by the black lines and genesis locations by black circles. The box indicates an area used for analysis.

Atlantic will be more constrained than areas away from inflow boundaries and this is explored in detail in section 3.

2.2. Ensemble Design

Ensemble members share the same lateral and lower boundary conditions that represent the external forcing, and IV is triggered by perturbations to the initial conditions. In an attempt to maximize ensemble spread, multiple methods are used to perturb the initial condition. This also allows us to explore the sensitivity of IV to initial perturbation type and amplitude.

The first method is a time-lagged approach using two different lags of 1 month (for four members starting on 1 January, 1 February, 1 March, and 1 April and collectively referred to hereafter as subensemble ENS_1M) and 6 h (for eight members starting on 29 April at 00, 06, 12, and 18 Z and on 30 April at 00, 06, 12, and 18 Z and collectively referred to hereafter as subensemble ENS_6H). The second method generates perturbations to the initial condition using a stochastic kinetic-energy backscatter scheme [*Berner et al*., 2011]. The backscatter scheme represents model uncertainty associated with missing subgrid scale dynamical process by randomly forcing the grid scale through the introduction of vorticity perturbations [*Shutts*, 2005]. Four ensemble members (collectively referred to hereafter as subensemble ENS_SB) are generated by initializing the model at 18 Z on 30 April and integrated forward with the backscatter scheme turned on for 6 h to generate four equally likely initial conditions at 00 Z on 1 May.

The ensemble (summarized in Table 1) therefore comprises 16 members all with different and equally likely initial conditions at 00 Z on 1 May 1998, and the entire ensemble is integrated forward 7 months through 1 December 1998. The initial conditions (not shown) show different synoptic patterns across subensemble ENS_1M, whereas for subensemble ENS_6H the start times fall within a synoptic timescale of initial time thereby limiting divergence between members. ENS_SB also has similar synoptic patterns between members for the same reason but with greater spread in the intensity of the synoptic systems than ENS_6H, as measured by the 500 hPa height (not shown).

2.3. Cyclone Tracking

Cyclones are identified and tracked using an objective tracking algorithm described in *Hodges* [1995, 1999] applied to 6-hourly data. Maxima in band-pass filtered 700 hPa relative vorticity are tracked above a threshold value of $10^{-5}\,s^{-1}$. The filter uses the 800–5000 km band to remove small-scale noise and the planetary wave signal and thus isolates the synoptic scales. Tracks are determined using a nearest neighbor approach that maximizes track smoothness. Tracks must extend longer than 2 days and 1000 km (following *Thorncroft and Hodges* [2001]).

TC parameters are extracted from a search radius of 1° about the 6-hourly track locations, and tracks are determined to be TCs if they satisfy warm core, duration, and intensity criteria following *Suzuki-Parker* [2012]. Warm core criteria are (1) the sum of temperature anomalies at 300, 500, and 700 hPa must be greater

Table 1. Summary of the Ensemble Members

Abbreviation	Method of Construction	Number of Members	Start Times
ENS_1M	1 month lag	4	1 Jan, 1 Feb, 1 Mar, 1 Apr
ENS_6H	6 h lag	8	29 Apr 00, 06, 12, 18 Z 30 Apr 00, 06, 12, 18 Z
ENS_SB	Backscatter scheme integrated for 6 h	4	30 Apr 18 Z

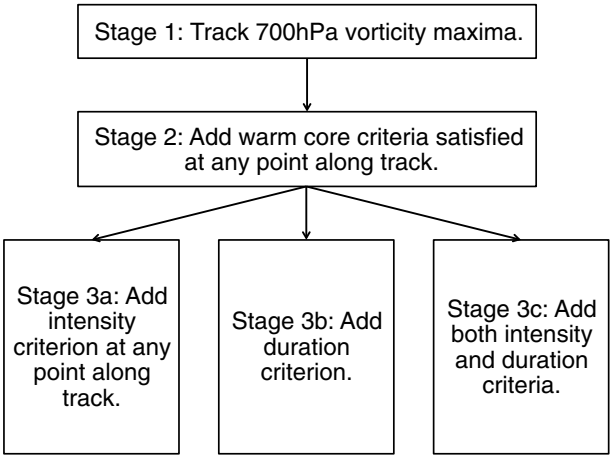

Figure 2. Flow chart describing the multistage feature tracking analysis.

than 0 K, (2) the temperature anomaly at 300 hPa must be greater than that at 850 hPa, and (3) 850 hPa wind speed must be greater than that at 300 hPa. A single duration criterion requires warm core criteria to be satisfied for not less than 2 days, and a single intensity criterion requires maximum wind speed at 10 m above the surface to be greater than 17 ms^{-1}.

2.4. Multistage Feature Tracking Analysis

Wu et al. [2012] incrementally added criteria to an objective tracking algorithm to determine at what stage in TC development IV arises over the northwest Pacific. We adopt a similar approach here applied to the 16-member ensemble of North Atlantic simulations specifically to identify potential physical sources of IV. Criteria are added sequentially in three stages (as outlined in Figure 2), and the ensemble spread of tracks is examined at each stage. Stage 1 simply considers vorticity tracks. Stage 2 adds warm core criteria. Stage 3 considers three different combinations of additional criteria: stage 3a adds the intensity criterion; stage 3b adds the duration criterion; and finally stage 3c adds both intensity and duration criteria.

3. Results

3.1. Internal Variability of the Summer Mean Environment

It is possible that the summer mean environment in the interior model domain may itself exhibit IV. The purpose of this study is to explore TC IV for a given climate state so it is important to ensure that ensemble members have the same mean environment before analyzing TC IV. Genesis potential indices [e.g., *Emanuel and Nolan*, 2004; *Bruyère et al*., 2012; *Menkes et al*., 2012] provide useful measures of the level of support provided by the summer mean environment for TC genesis. The Cyclone Genesis Index (CGI) was developed by *Bruyère et al*. [2012] specifically for the North Atlantic and is used here to characterize the summer mean environment. The CGI comprises potential intensity [*Emanuel*, 1995] and vertical wind shear, and taking summer mean (August-September-October) values averaged over a subregion of the tropical North Atlantic (5°–20°N, 60°–15°W) offers the highest correlation to TC frequency for the entire season and North Atlantic basin [*Bruyère et al*., 2012].

A normalized measure of variability is given by the ensemble standard deviation divided by the ensemble mean, known as the coefficient of variation (CV). The ensemble CV of summer mean CGI averaged over the tropical North Atlantic subregion is 0.02 indicating that CGI varies by 2% of the ensemble mean. To determine the relative importance of this variability, it is instructive to compare with the interannual variability across a recent 30 year period (1981–2010) calculated using reanalysis data (National Centers for Environmental Prediction-National Center for Atmospheric Research (NCAR) Reanalysis Project [*Kalnay et al*., 1996]). The interannual CV is an order of magnitude larger at 0.26 suggesting that the summer mean environment can be considered the same for each ensemble member. Furthermore, a linear regression between observed TC frequency for the whole season and North Atlantic basin and CGI over the 30 year period indicates that a change in CGI of 0.015 is needed to change the TC frequency by a single storm. Given that the ensemble standard deviation of CGI is approximately half that value at 0.007, it is unlikely that the ensemble spread in the summer mean environment contributes significantly to the ensemble spread in TC frequency. Finally, the range in the subensemble (ENS_1M, ENS_6H, and ENS_SB) means is also small at 0.006. This analysis shows that the summer mean environment is insensitive to both the initial condition perturbation and the perturbation method.

Table 2. Results of the Multistage Feature Tracking Analysis Showing the Numbers of Tracks Starting South of 21°N and East of 62°W (Subregion Indicated in Figure 1)[a]

	Stage 1: Vorticity Maxima	Stage 2: + Warm Core	Stage 3a: + Intensity	Stage 3b: + Duration	Stage 3c: + Intensity and Duration
Ensemble mean	55.1	22.1	13.9	11.3	8.8
Ensemble range	43–64	18–26	11–17	8–14	6–12
Ensemble standard deviation	5.6	2.6	1.7	1.6	1.9
Coefficient of variation[b]	0.10	0.12	0.12	0.14	0.22

[a]Adapted from *Holland et al*. [2014]. Copyright 2014, Offshore Technology Conference. Reproduced with permission of OTC. Further reproduction prohibited without permission.
[b]The coefficient of variation is the ensemble standard deviation divided by the ensemble mean.

3.2. Multistage Feature Tracking Analysis

To isolate and understand IV of TCs that develop from easterly waves, the multistage feature tracking analysis is restricted to tracks starting south of 21°N and east of 62°W (the subregion indicated in Figure 1).

The 16-member ensemble produces a range in May through December TC frequency for the subregion of 6 to 12 storms with an ensemble mean of 8.8 and a standard deviation of 1.9, resulting in a CV of 0.22. TC frequency therefore exhibits substantial IV that amounts to 22% of the ensemble mean. For comparison, the observed interannual range in TC frequency for the subregion over the recent 30 year period (1981–2010) is 0 to 10 with a mean of 4.7 and standard deviation of 2.7 resulting in a CV of 0.57, using IBTrACS data [*Knapp et al*., 2010]. The simulated IV of TC frequency for 1998 is therefore 39% (0.22/0.57 = 0.39) of the total (externally forced and internal) observed variability of TC frequency. We note, however, that our case study year 1998 was a year of above average TC frequency with 7 TCs observed in the subregion and other years may exhibit quite different IV.

Results of the multistage feature tracking analysis (Table 2) show that adding criteria increases the IV of track frequency and therefore shows the growth of IV at each stage of TC development. Vorticity tracks (stage 1) exhibit 45% (0.1/0.22 = 0.45) of the IV of TCs (stage 3c). Adding warm core criteria to the vorticity tracks only contributes another 9% toward the IV of TCs. Combining intensity and warm core criteria does not increase IV further, and combining duration and warm core criteria only adds another 9%. Finally, combining all criteria (intensity, duration, and warm core) contributes the final 37% of TC IV. For easterly wave developments then, this analysis shows that almost half the IV of TCs may be attributed to the waves themselves and almost half again may be attributed to the attainment of intense *and* long-lived warm cores (i.e., TCs). Given that the location of the eastern domain boundary was chosen to provide each ensemble member with the same wave activity at the African coast, the ensemble does not account for the contributions of upstream wave variability to TC IV. The contribution of waves to TC IV in the ensemble is therefore likely to be a conservative estimate.

3.3. Sources of Internal Variability

The multistage feature tracking analysis provides clues as to the possible physical mechanisms through which IV of TCs operates. We focus on the two stages of TC development that contributed most to their IV, that is, first the initial vorticity tracks and second the transition to long-lived *and* intense warm cores.

3.3.1. Internal Variability of Vorticity Tracks

Here we explore how IV of easterly waves arises within the limited area domain that has wave activity prescribed at the eastern domain boundary. *Crétat et al*. [2011] defined a metric known as the reproducible fraction (RF) to quantify IV at the daily timescale. RF quantifies the fraction of day-to-day variability that occurs in phase between ensemble members. RF is defined as the ratio of the daily variance of the ensemble mean across the daily data (*n* days) to the variance of the ensemble members (*n* days reproduced 16 times).

Here RF is calculated on 6-hourly data, and Figure 3 shows RF of 700 hPa relative vorticity over the summer season (August-September-October). Values equal to 1 indicate that all variability is in phase between members and values of 0 indicate that none of the variability is in phase. As expected, RF is high at the domain boundaries and lower in the domain interior. High values extend farthest into the domain at the inflow boundaries, with high values extending across the tropical North Atlantic decreasing toward the

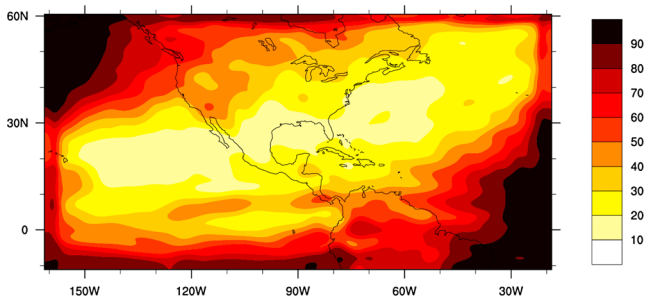

Figure 3. Reproducible fraction of 700 hPa relative vorticity (%) for August-September-October.

Caribbean. This demonstrates the changeover from boundary forced constancy to IV east to west across the tropical North Atlantic.

The majority of vorticity tracks start at the eastern boundary with a smaller number of tracks starting within the domain interior across the tropical North Atlantic (Figure 4b). However, the standard deviation of vorticity track start points is similar across the entire tropical North Atlantic (Figure 4d). Vorticity tracks that start within the domain interior are therefore more variable than those starting at the eastern boundary, as expected, and is consistent with the west to east decrease in RF (Figure 3). This behavior is reflected in the vorticity track density (Figures 4a and 4c) and raises the question of what controls the rate of increase of IV east to west.

To further understand the IV of vorticity tracks, we perform an analysis at the individual track level. A crude measure of the variability of track occurrence is the daily count of tracks across all ensemble members east of 30°W (shown in Figure 5). A count close to the ensemble size of 16 implies that almost all ensemble members

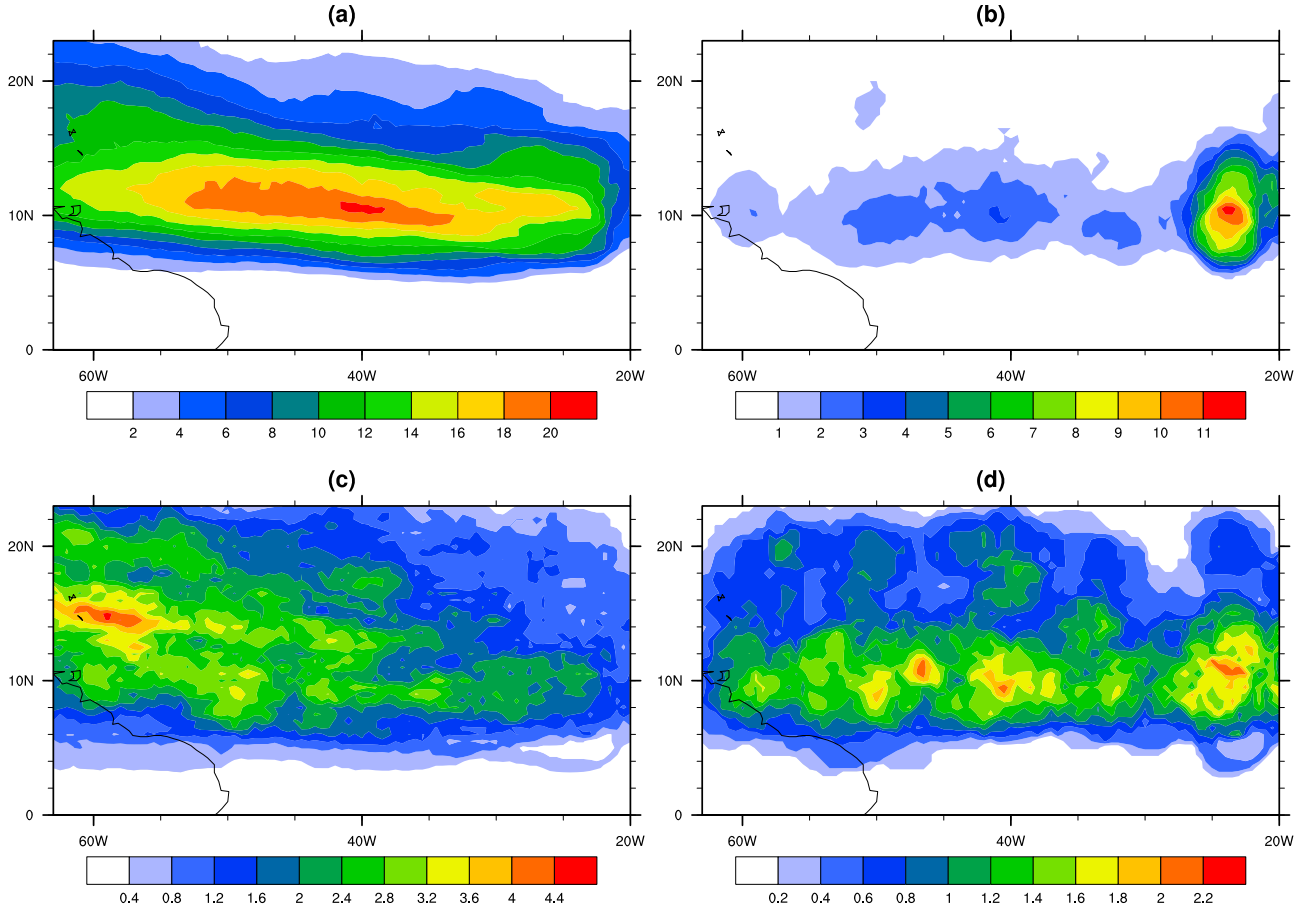

Figure 4. (a) Ensemble mean vorticity track density, (b) ensemble mean vorticity track start point density, (c) ensemble standard deviation of vorticity track density, and (d) ensemble standard deviation of vorticity track start point density. All plots are for the period August-September-October. Density is defined as the number of vorticity track points within a 2.5° radius circle. Adapted from *Holland et al.* [2014]. Copyright 2014, Offshore Technology Conference. Reproduced with permission of OTC. Further reproduction prohibited without permission.

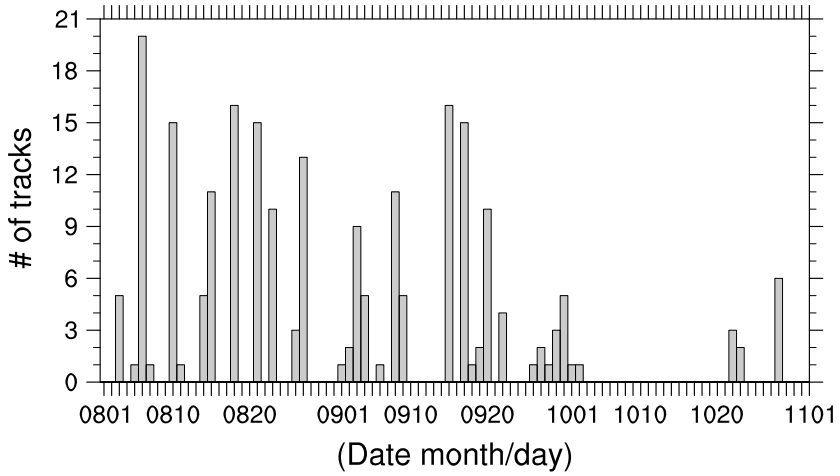

Figure 5. Ensemble daily total number of vorticity tracks forming east of 30°W for the period August-September-October. Adapted from *Holland et al.* [2014]. Copyright 2014, Offshore Technology Conference. Reproduced with permission of OTC. Further reproduction prohibited without permission.

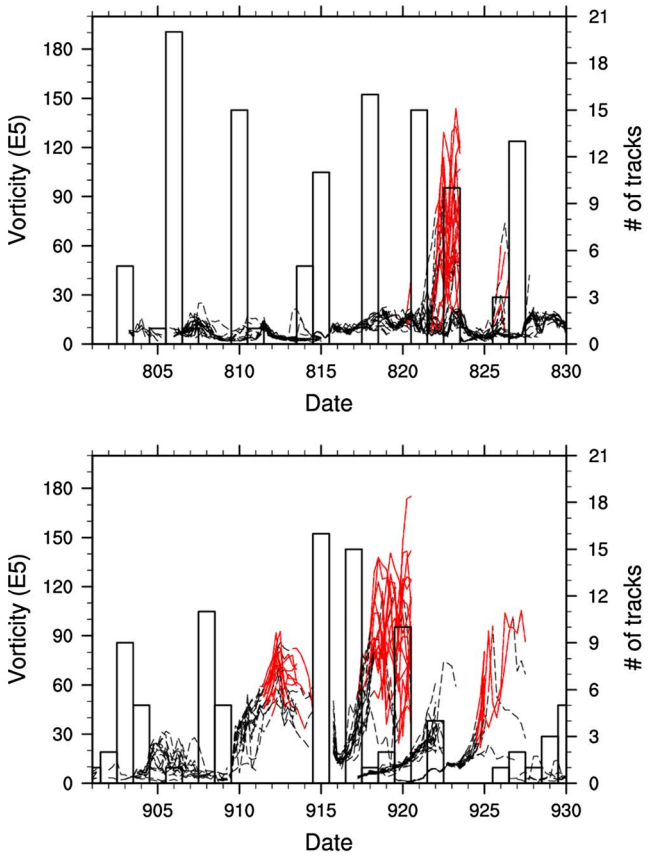

Figure 6. As for Figure 5 but with the addition of 5 day vorticity-time trajectories of the subsequent tracks for August (top) and September (bottom). Trajectories change from black dashed line to red solid line when TC criteria (warm core and intensity but not duration) are satisfied. Adapted from *Holland et al.* [2014]. Copyright 2014, Offshore Technology Conference. Reproduced with permission of OTC. Further reproduction prohibited without permission.

may contain a track although there will be some scatter due to some members developing the wave later or sooner and counted in an adjacent day. There is also the possibility that some members contain two tracks within a 24 h period. In general, though, Figure 5 clearly shows that vorticity tracks exhibit IV and the magnitude of the IV is different for each track.

Expanding upon this analysis, it is instructive to analyze the subsequent time-vorticity trajectories (Figure 6). The IV of track occurrence is indicated by the daily track count (bars in Figure 6), and the IV of track development to a TC (warm core and intensity criteria satisfied) is indicated by the resulting time-vorticity trajectories. The magnitude of the IV of both track occurrence and track development is different for each track. There are tracks that occur in almost every ensemble member, and all do not develop into TCs (e.g., 6, 10, and 14–15 August); tracks that occur in almost every ensemble member, and all develop into TCs (8–9 and 15 September); tracks that only occur in a few ensemble members, and all do not develop (August 3); and finally, tracks that only occur in a few ensemble members, and only some of those

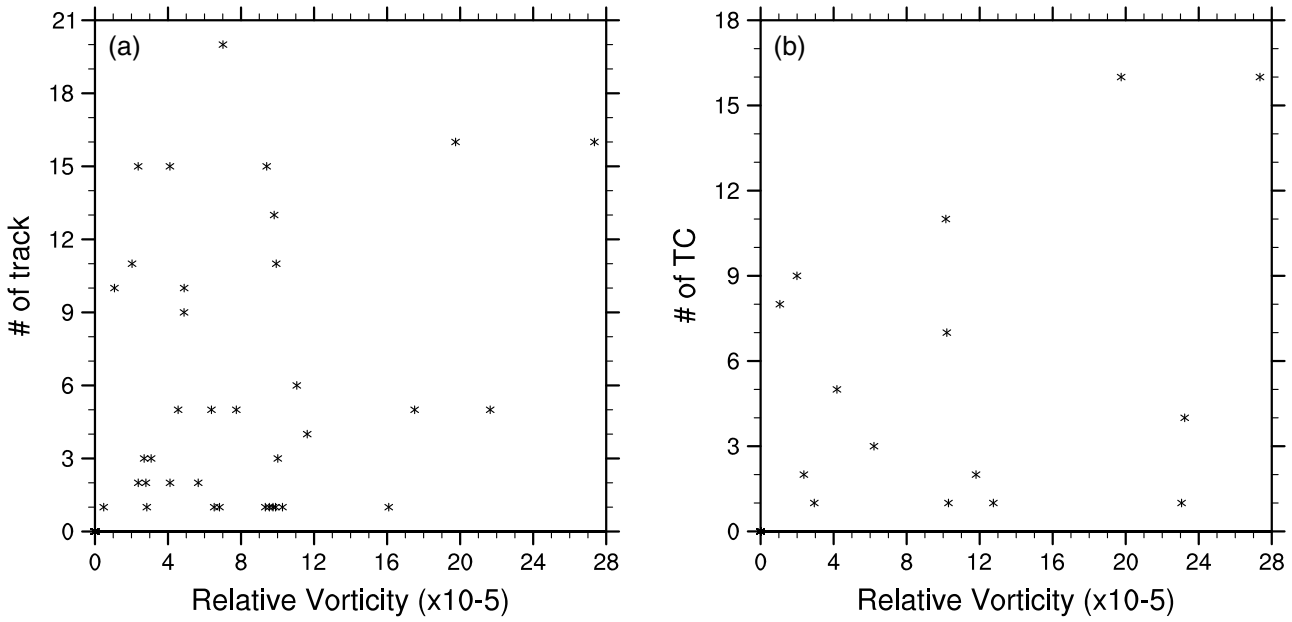

Figure 7. Scatter plot of (a) daily ensemble total number of tracks east of 30°W versus average vorticity of the daily tracks east of 30°W ($r^2 = 0.33$) and (b) daily ensemble total number of tracks east of 30°W that go on to develop into TCs versus average vorticity of the daily tracks ($r^2 = 0.49$).

develop in TCs (20 September). Interestingly, we do not see cases where tracks occur in a few members yet all develop into TCs.

To explore the relationship between wave occurrence and wave amplitude further, Figure 7a shows only a weak relationship between predictability of occurrence (as measured by the ensemble daily total number of tracks) and wave amplitude (as measured by the daily average vorticity over the tracks) with only 33% of the variance explained (significant at 99% using a two-sided test). On the other hand Figure 7b indicates a higher correlation between wave amplitude and predictability of development into a TC with 49% of the variance explained (significant at 99% using a two-sided test). This positive correlation between wave amplitude and variability of development to a TC implies that the stochastic component of the development process is progressively reduced as wave strength increases.

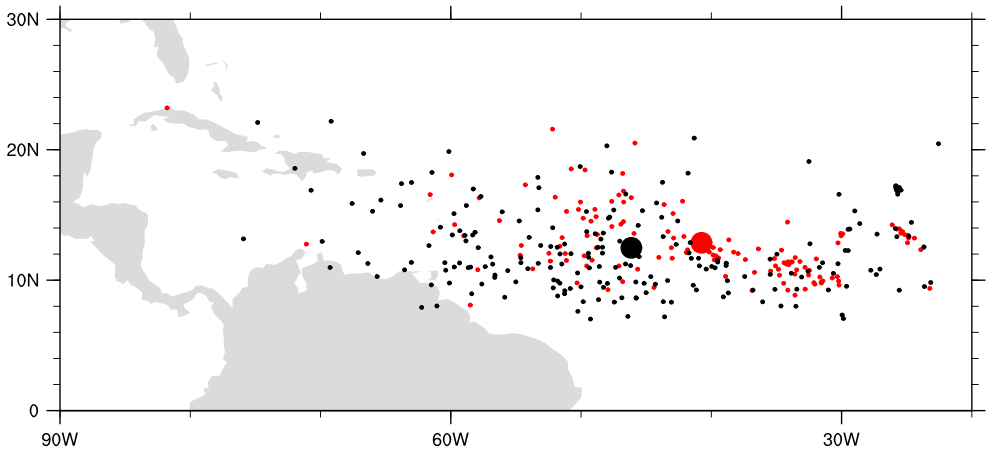

Figure 8. Locations of the first track points that meet warm core criteria across all ensemble members for tracks that develop into TCs (red) and tracks that do not develop into TCs (black). The large dots indicate the mean location of the two populations.

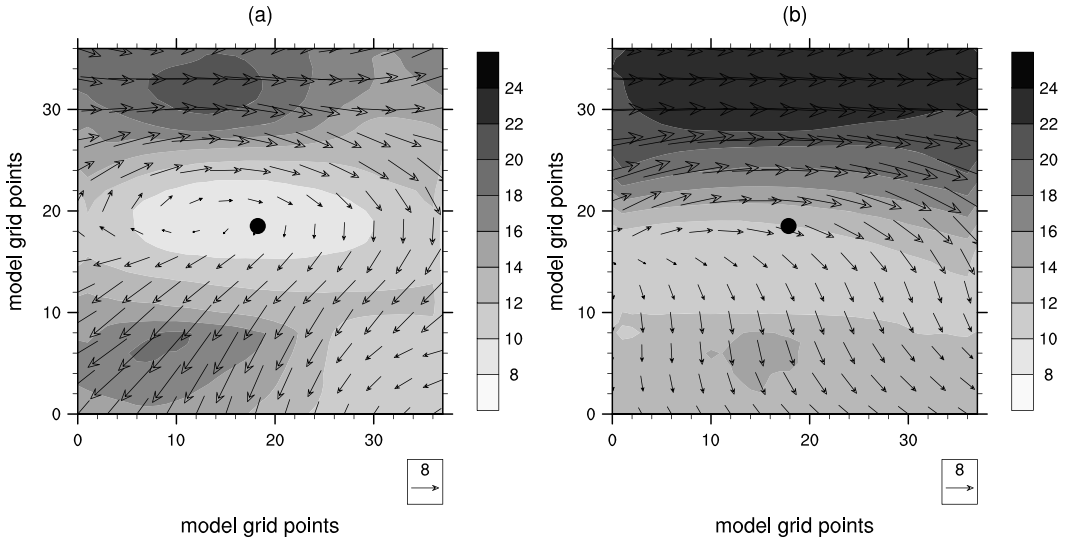

Figure 9. Composite environment wind shear (shading, ms^{-1}) and wind shear vectors constructed by removing the signatures of the tropical cyclones following *Davis et al.* [2008a] for (a) developing warm cores and (b) nondeveloping warm cores. The black dots indicate the composite cyclone centers, and the approximate dimensions of the region shown are 1368 km × 1368 km. Adapted from *Holland et al.* [2014]. Copyright 2014, Offshore Technology Conference. Reproduced with permission of OTC. Further reproduction prohibited without permission.

3.3.2. Internal Variability of Tropical Cyclones

Almost half the IV of mature TCs arises from the addition of both intensity and duration criteria. This portion of IV therefore arises at the stage in cyclone development from the initial warm core to one that has a persistent and strong surface circulation. Here we explore the role of the synoptic environment. The potential importance of local cyclone factors is discussed in the next section.

The geographic spread of locations of developing and nondeveloping warm cores (Figure 8) shows that developing cores have a tendency to form farther east than nondeveloping cores. Developing cores may therefore be located in a different environment on average than nondeveloping cores. Potentially important large-scale environmental variables include wind shear and potential intensity. Since potential intensity is highly correlated with SST and the underlying SST does not vary between ensemble members, potential intensity does not vary significantly across the ensemble (not shown). A more likely controlling factor is wind shear. The composite environmental shear, calculated using the TC removal technique of *Davis et al.* [2008a], about developing and nondeveloping warm cores (Figure 9) confirms that the composite developing warm core is located in a favorable minimum in shear of 6 ms^{-1}, whereas the composite nondeveloping warm core is located in a more unfavorable westerly shear of 10–12 ms^{-1}.

The upper level flow over the tropical North Atlantic varies across the ensemble on synoptic timescales (not shown). Shear variability between ensemble members could therefore be a source of TC IV. Shear associated with synoptic systems may vary due to ensemble spread in the synoptic systems themselves and also due to differences in the timing and locations of the warm cores that therefore experience different synoptic environments. The August mean ensemble mean 200 hPa height (Figure 10a) shows a characteristic tropical upper tropospheric trough (TUTT) axis extending northeast-southwest across the North Atlantic. The corresponding RF (Figure 10b) shows values less than 0.3 in the region of the TUTT due to transient cyclonic centers that track southwest along the trough axis and vary in timing and intensity between ensemble members (not shown). The TUTT brings high shear to low latitudes over the North Atlantic (Figure 10c) with correspondingly low RF less than 0.3 (Figure 10d) indicating highly variable shear across the ensemble on synoptic timescales.

4. Discussion

This section discusses limitations of the study, with particular focus on the constraints imposed by using a limited area domain, and highlights other potentially important contributions to TC IV.

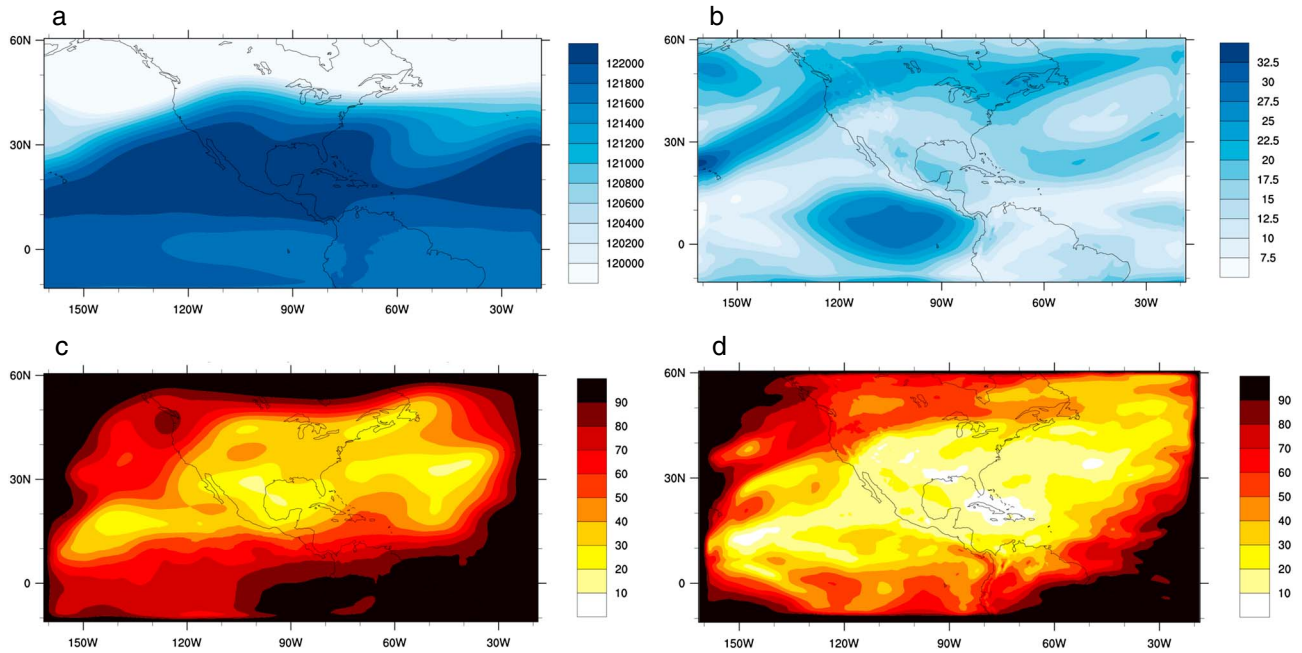

Figure 10. (a) Ensemble mean August mean 200 hPa height (m), (b) ensemble mean August mean wind shear (ms^{-1}), (c) reproducible fraction of August 200 hPa height (%), and (d) reproducible fraction of August wind shear (%).

The experimental design was necessarily constrained by computational resources that introduced a number of limitations. Simulated IV is likely to be a lower bound on IV in the real world due to numerical constraints including finite resolution, numerical diffusion, and physics parameterizations. *Crétat et al*. [2011], for example, showed IV of rainfall over South Africa to be dependent on the convection parameterization scheme used. Resolving deep convection in particular may produce markedly different IV of TC frequency than the IV reported here using a 36 km grid. Perhaps the most serious constraint is the lack of accounting for processes outside the limited area domain that may contribute to IV within the domain. In particular, the location of the eastern domain boundary results in all ensemble members having the same easterly jet, wave structure, and amplitude at the eastern boundary and effectively removes potential contributions of IV in wave activity associated with barotropic and baroclinic instability along the African easterly jet. Another potentially severe limitation is lack of accounting for IV arising from coupled atmosphere-ocean processes. Potential sources of IV may occur at the individual cyclone scale through wind-driven mixing and cooling of the ocean under a cyclone that can feedback to weaken the cyclone, as simulated by *Davis et al*. [2008b], and also at the seasonal scale as subsequent cyclones are influenced by the cool wakes of earlier storms [*Hart*, 2010]. Global variable resolution meshes and coupled atmosphere-ocean models offer a potential solution to many of these constraints and are being explored in a follow-on study.

The changeover from boundary forced constancy to IV east to west across the tropical North Atlantic (shown previously in Figure 3) may arise from internal nonlinear processes associated with deep convection [e.g., *Shutts and Palmer*, 2007; *Berner et al*., 2011], 2-D turbulence processes including upscale developments from vortex interaction [e.g., *Holland*, 1995], or variable midlatitude interactions [e.g., *Bosart and Bartlo*, 1991; *Davis and Bosart*, 2003]. The 36 km grid used here is not well suited to explore contributions from processes that operate on convective spatial scales and may even misrepresent their contributions to TC IV. Investigations at higher resolution could elucidate some of these potentially important mechanisms.

The investigation into the potential physical sources of IV of TC frequency identified variable vertical wind shear as a potentially important contributing factor. Specifically, evidence is provided that the variable transition to long-lived *and* intense vortices may be controlled by variable shear environments arising from highly variable TUTT lows, the transient component of TUTTs [*Ferreira and Schubert*, 1999]. TUTT variability is known to arise due to nonlinear interactions between radiation and water vapor [*Sadler*, 1976, 1978]. The factors that determine whether a TC develops in conjunction with a TUTT low are not well known (T. J. Galarneau Jr. et al., Development of North Atlantic tropical disturbances near upper level

potential vorticity streamers, submitted to *Journal of the Atmospheric Sciences*, 2014), but TUTTs are thought to both promote and inhibit TC development depending on the relative positions and intensities of the TUTT and TC [*Patla et al*., 2009]. Inhibition may occur through vertical wind shear [*DeMaria et al*., 2001], whereas development may be aided through quasi-geostrophic ascent through a deep layer associated with the upper level low (Galarneau et al., submitted manuscript, 2014) and enhanced divergence aloft [*Davis and Bosart*, 2004].

As mentioned in section 3, variable interactions between developing TCs and TUTT lows is one of many potentially important mechanisms for the generation of TC IV. However, given that the oceanic boundary conditions are identical in each ensemble member, it seems unlikely that environmental thermal energy contributed significantly to IV. Midlevel moisture, on the other hand, may be important but was not explored here. Other potentially important factors not considered here include small-scale convective nonlinearities, even in a parameterized sense, and mesoscale vortex interactions and upscaling as suggested by *Jourdain et al*. [2011]. However, the 36 km grid is not well suited for such exploration and may misrepresent the contributions of convective processes to TC IV.

5. Conclusions

Using a regional model initial condition ensemble experiment, this study has quantified the magnitude of IV of North Atlantic TC frequency for a single case study year and identified potential physical sources. The summer mean environment is similar for each ensemble member and is also insensitive to both the initial condition perturbation and the perturbation method. Variability in the large-scale environment does not therefore contribute to ensemble spread in TC frequency, and the spread can be solely attributed to internal variability.

The ensemble produced a large spread in TC frequency over the tropical North Atlantic with a range of 6 to 12 storms. The normalized ensemble variability (defined as the standard deviation divided by the mean) of 0.22 is approximately two fifths the magnitude of the observed total interannual variability over a recent 30 year period indicating that TC frequency exhibits substantial IV. However, this result is based on a single active season and may not be representative of other years. Other studies indicate that IV of TC frequency is dependent on the external forcing and is therefore likely to vary by year [e.g., *Chen and Lin*, 2013; *Wu et al*., 2012; *Au-Yeung and Chan*, 2012]. An interesting extension to this work would be to conduct a similar ensemble analysis across other seasons and basins to explore relationships between IV and large-scale forcing.

A multistage feature tracking analysis over the tropical North Atlantic showed that IV of TC frequency arises in approximately equal measure from the occurrence and development of easterly waves and the transition of warm cores to long-lived *and* intense vortices (i.e., TCs). The interim development stage from a wave to an established warm core, often considered being a highly stochastic process due to the prevalence of deep convection and vortex mergers, did not contribute appreciably to the IV of TC frequency. Indeed, this transition stage only contributed 9% to the total TC IV. In contrast, *Wu et al*. [2012] found very little IV even at the late stage of established warm core systems and found most IV of TC frequency to arise from the transition from short-lived to long-lived warm cores rather than also during intensification as found in this study. Many factors likely play a role in explaining this differing result such as details of model setup and geographic location, not least perhaps the difference in the large-scale environment and genesis pathways between the tropical North Atlantic and northwest Pacific.

Variability in the occurrence and development of easterly waves is found to be wave-dependent with some waves exhibiting very little variability, while others were highly variable. A significant positive correlation is found between wave occurrence and development and wave strength, and this may be related to the ability of stronger incipient vortices to persist and develop in marginally favorable environments.

Variability in the synoptic environment is identified as contributing to variability in the transition from warm cores to long-lived and intense vortices. The synoptic environment differs between the ensemble members due to both different locations of the initial warm cores and synoptic variability at the upper levels. Given that the environment is characterized by the same thermal energy (the same SSTs), it is likely that the dominant differences are dynamical and shear due to TUTT variability is shown to be a controlling factor.

These results are in agreement with *Zhang and Tao* [2013], who showed that environmental shear has a strong influence on the predictability of TC formation.

A consequence of IV is an upper limit on the predictability of seasonal TC frequency. Indeed, this study finds that a plausible lower limit for the magnitude of IV for the year 1998 is 40% of the total interannual variability of TC frequency. Should other years exhibit similar nonnegligible magnitudes of IV, this has implications for the interpretation of seasonal TC forecasts that make the implicit assumption that the externally forced component is far larger than the internal component. Ensemble-based forecasts, as explored by *Chen and Lin* [2013], are therefore preferable to isolate the predictable component. However, since IV is an intrinsic property of the real atmosphere, this too will likely differ from the predicted ensemble mean, even for a perfect model, implying an upper limit for seasonal predictability, and possible explanation for the poor forecast of the 2013 North Atlantic hurricane season [*Vecchi and Villarini*, 2014]. Similarly, empirical downscaling methods that tie TC frequency to large-scale environment variables [e.g., *Emanuel and Nolan*, 2004; *Bruyère et al*., 2012; *Menkes et al*., 2012] are limited by the presence of IV in the proportion of total variance that can be explained. Both the production and evaluation of seasonal forecasts and empirical downscaling may benefit from an explicit inclusion of the potential limitations arising from IV. Finally, risk management may benefit from a quantification of the proportion of seasonal TC losses that is fundamentally not predictable by devising strategies to optimally manage the externally forced (predictable) and internal (unpredictable) losses.

Acknowledgments
This work benefitted from comments from three anonymous reviewers. NCAR is supported by the National Science Foundation, and this work was partially supported by the Willis Research Network, the Research Partnership to Secure Energy for America, the Climatology and Simulation of Eddies/Eddies Joint Industry Project, and NSF EaSM grants AGS-1048841 and AGS-1048829. All data generated through this work are freely available by contacting the corresponding author.

References

Alexandru, A., R. de Elia, and R. Laprise (2007), Internal variability in regional climate downscaling at the seasonal scale, *Mon. Weather Rev.*, *135*, 3221–3238, doi:10.1175/MWR3456.1.

Au-Yeung, A. Y. M., and J. C. L. Chan (2012), Potential use of a regional climate model in seasonal tropical cyclone activity predictions in the western North Pacific, *Clim. Dyn.*, *39*(3-4), 783–794, doi:10.1007/s00382-011-1268-x.

Berner, J., S.-Y. Ha, J. P. Hacker, A. Fournier, and C. Snyder (2011), Model uncertainty in a mesoscale ensemble prediction system: Stochastic versus multiphysics representations, *Mon. Weather Rev.*, *139*, 1972–1995, doi:10.1175/2010MWR3595.1.

Bosart, L. F., and J. A. Bartlo (1991), Tropical storm formation in a baroclinic environment, *Mon. Weather Rev.*, *119*, 1979–2013, doi:10.1175/1520-0493(1991)119<1979:TSFIAB>2.0.CO;2.

Bruyère, C. L., G. J. Holland, and E. Towler (2012), Investigating the use of a genesis potential index for tropical cyclones in the North Atlantic basin, *J. Clim.*, *25*, 8611–8626, doi:10.1175/JCLI-D-11-00619.1.

Caya, D., and S. Biner (2004), Internal variability of RCM simulations over an annual cycle, *Clim. Dyn.*, *22*, 33–46, doi:10.1007/s00382-003-0360-2.

Chen, F., and J. Dudhia (2001), Coupling an advanced land-surface/ hydrology model with the Penn State/NCAR MM5 modeling system. Part I: Model implementation and sensitivity, *Mon. Weather Rev.*, *129*, 569–585, doi:10.1175/1520-0493(2001)129<0569:caalsh>2.0.co;2.

Chen, J.-H., and S.-J. Lin (2011), The remarkable predictability of inter-annual variability of Atlantic hurricanes during the past decade, *Geophys. Res. Lett.*, *38*, L11804, doi:10.1029/2011GL047629.

Chen, J.-H., and S.-J. Lin (2013), Seasonal predictions of tropical cyclones using a 25-km-resolution general circulation model, *J. Clim.*, *26*, 380–398, doi:10.1175/JCLI-D-12-00061.1.

Christensen, O. B., M. A. Gaertner, J. A. Prego, and J. Polcher (2001), Internal variability of regional climate models, *Clim. Dyn.*, *17*, 875–887, doi:10.1007/s003820100154.

Collins, W. D., et al. (2006), The community climate system model version 3 (CCSM3), *J. Clim.*, *19*, 2122–2143, doi:10.1175/JCLI3761.1.

Crétat, J., C. Macron, B. Pohl, and Y. Richard (2011), Quantifying internal variability in a regional climate model: A case study for Southern Africa, *Clim. Dyn.*, *37*(7-8), 1335–1356, doi:10.1007/s00382-011-1021-5.

Davis, C. A., and L. F. Bosart (2003), Baroclinically induced tropical cyclogenesis, *Mon. Weather Rev.*, *131*, 2730–2747, doi:10.1175/1520-0493(2003)131<2730:BITC>2.0.CO;2.

Davis, C. A., and L. F. Bosart (2004), The TT problem, *Bull. Am. Meteorol. Soc.*, *85*, 1657–1662, doi:10.1175/BAMS-85-11-1657.

Davis, C. A., C. Snyder, and A. C. Didlake (2008a), A vortex-based perspective of eastern Pacific tropical cyclone formation, *Mon. Weather Rev.*, *136*, 2461–2477, doi:10.1175/2007MWR2317.1.

Davis, C. A. W., et al. (2008b), Prediction of landfalling hurricanes with the advanced hurricane WRF model, *Mon. Weather Rev.*, *136*, 1990–2005, doi:10.1175/2007MWR2085.1.

DeMaria, M., J. A. Knaff, and B. H. Conell (2001), A tropical cyclone genesis parameter for the tropical Atlantic, *Weather Forecast.*, *16*, 219–233, doi:10.1175/1520-0434(2001)016<0219:ATCGPF>2.0.CO;2.

Deser, C., A. S. Phillips, V. Bourdette, and H. Teng (2012), Uncertainty in climate change projections: The role of internal variability, *Clim. Dyn.*, *38*, 527–546, doi:10.1007/s00382-010-0977-x.

Deser, C., A. S. Phillips, M. A. Alexander, and B. V. Smoliak (2013), Projecting North American climate over the next 50 years: Uncertainty due to internal variability, *J. Clim.*, *27*, 2271–2296, doi:10.1175/JCLI-D-13-00451.1.

Diaconescu, E. P., R. Laprise, and A. Zadra (2012), Singular vectors decomposition of the internal variability of the Canadian Regional Climate Model, *Clim. Dyn.*, *38*(5-6), 1093–1113, doi:10.1007/s00382-011-1179-x.

Done, J. M., G. J. Holland, C. L. Bruyère, L. R. Leung, and A. Suzuki-Parker (2013), Modeling high-impact weather and climate: Lessons from a tropical cyclone perspective, *Clim. Change*, doi:10.1007/s10584-013-0954-6, in press.

Emanuel, K. A. (1995), Sensitivity of tropical cyclones to surface exchange coefficients and a revised steady-state model incorporating eye dynamics, *J. Atmos. Sci.*, *52*, 3969–3976, doi:10.1175/1520-0469(1995)052<3969:SOTCTS>2.0.CO;2.

Emanuel, K. A., and D. S. Nolan (2004), Tropical cyclone activity and global climate, Preprints, 26th Conf. on Hurricanes and Tropical Meteorology, Miami, FL, 240–241, Am. Meteorol. Soc.

Ferreira, R. N., and W. H. Schubert (1999), The role of tropical cyclones in the formation of tropical upper-tropospheric troughs, *J. Atmos. Sci.*, *56*, 2891–2907, doi:10.1175/1520-0469(1999)056<2891:TROTCI>2.0.CO;2.

Giorgi, F., and X. Bi (2000), A study of internal variability of a regional climate model, *J. Geophys. Res.*, *105*, 29,503–29,521, doi:10.1029/2000JD900269.

Giorgi, F., M. R. Marinucci, G. T. Bates, and G. D. Canio (1993), Development of a second-generation Regional Climate Model (RegCM2). Part II: Convective processes and assimilation of lateral boundary conditions, *Mon. Weather Rev.*, *121*, 2814–2832, doi:10.1175/1520-0493(1993)121<2794:DOASGR>2.0.CO;2.

Hart, R. E. (2010), An inverse relationship between aggregate tropical cyclone activity and subsequent winter climate, *Geophys. Res. Lett.*, *38*, L01705, doi:10.1029/2010GL045612.

Hawkins, E., and R. Sutton (2009), The potential to narrow uncertainty in regional climate predictions, *Bull. Am. Meteorol. Soc.*, *90*, 1095–1107, doi:10.1175/2009BAMS2607.1.

Hawkins, E., and R. Sutton (2010), The potential to narrow uncertainty in projections of regional precipitation change, *Clim. Dyn.*, *37*, 407–418, doi:10.1007/s00382-010-0810-6.

Hodges, K. I. (1995), Feature tracking on the unit sphere, *Mon. Weather Rev.*, *123*, 3458–3465, doi:10.1175/1520-0493(1995)123<3458:FTOTUS>2.0.CO;2.

Hodges, K. I. (1999), Adaptive constraints for feature tracking, *Mon. Weather Rev.*, *127*, 1362–1373, doi:10.1175/1520-0493(1999)127<1362:ACFFT>2.0.CO;2.

Holland, G. J. (1995), Scale interaction in the western Pacific monsoon, *Meteorol. Atmos. Phys.*, *56*, 57–79, doi:10.1007/BF01022521.

Holland, G. J., J. M. Done, and C. L. Bruyere (2014), Assessing uncertainty and predictability of regional climate, with a focus on hurricanes. Paper OTC 25355 presented at the Offshore Technology Conference, Houston, Texas, 5–8 May, doi:10.4043/25355-MS.

Hong, S.-Y., and J.-O. J. Lim (2006), The WRF single-moment 6-class microphysics scheme (WSM6), *J. Korean Meteorol. Soc.*, *42*, 129–151.

Hong, S.-Y., and H.-L. Pan (1996), Nonlocal boundary layer vertical diffusion in a medium-range forecast model, *Mon. Weather Rev.*, *124*(10), 2322–2239, doi:10.1175/1520-0493(1996)124<2322:NBLVDI>2.0.CO;2.

Jourdain, N. C., P. Marchesiello, C. E. Menkes, J. Lefevre, E. M. Vincent, M. Lengaigne, and F. Chauvin (2011), Mesoscale simulation of tropical cyclones in the South Pacific: Climatology and interannual variability, *J. Clim.*, *24*, 3–25, doi:10.1175/2010JCLI3559.1.

Kain, J. S., and J. M. Fritsch (1990), A one-dimensional entraining/detraining plume model and its application in convective parameterization, *J. Atmos. Sci.*, *47*, 2784–2802, doi:10.1175/1520-0469(1990)047<2784:AODEPM>2.0.CO;2.

Kalnay, E., et al. (1996), The NCEP/NCAR 40-year reanalysis project, *Bull. Am. Meteorol. Soc.*, *77*, 437–477, doi:10.1175/1520-0477(1996)077<0437:TNYRP>2.0.CO;2.

Knapp, K., M. Kruk, D. Levinson, H. Diamond, and C. Neumann (2010), The International Best Track Archive for Climate Stewardship (IBTrACS) unifying tropical cyclone data, *Bull. Am. Meteorol. Soc.*, *91*, 363–376, doi:10.1175/2009BAMS2755.1.

Laprise, R., et al. (2012), Considerations of domain size and large-scale driving for nested regional climate models: Impact on internal variability and ability at developing small-scale details, in *Climate Change: Inferences from Paleoclimate and Regional Aspects*, edited by A. Berger, and F. Mesinger, D. Šijači, vol. 4, pp. 201–214, Springer, Vienna, Austria, doi:10.1007/978-3-7091-0973-1_14.

Leduc, M., and R. Laprise (2009), Regional climate model sensitivity to domain size, *Clim. Dyn.*, *32*, 833–854, doi:10.1007/s00382-008-0400-z.

Liang, X. Z., K. E. Kunkel, and A. N. Samel (2001), Development of a regional climate model for U.S. Midwest applications. Part I: Sensitivity to buffer zone treatment, *J. Clim.*, *14*, 4363–4378, doi:10.1175/1520-0442(2001)014<4363:DOARCM>2.0.CO;2.

Lucas-Picher, P., D. Caya, R. de Elia, and R. Laprise (2008), Investigation of regional climate models' internal variability with a ten-member ensemble of 10-year simulations over a large domain, *Clim. Dyn.*, *31*, 927–940, doi:10.1007/s00382-008-0384-8.

Menkes, C. E., M. Lengaigne, P. Marchesiello, N. C. Jourdain, E. M. Vincent, J. Lefèvre, F. Chauvin, and J.-F. Royer (2012), Comparison of tropical cyclogenesis indices on seasonal to interannual timescales, *Clim. Dyn.*, *38*, 301–321, doi:10.1007/s00382-011-1126-x.

Nikiéma, O., and R. Laprise (2011a), Diagnostic budget study of the internal variability in ensemble simulations of the Canadian RCM, *Clim. Dyn.*, *36*(11), 2313–2337, doi:10.1007/s00382-010-0834-y.

Nikiéma, O., and R. Laprise (2011b), Budget study of the internal variability in ensemble simulations of the Canadian RCM at the seasonal scale, *J. Geophys. Res.*, *116*, D16112, doi:10.1029/2011JD015841.

Nikiéma, O., and R. Laprise (2013), An approximate energy cycle for inter-member variability in ensemble simulations of a regional climate model, *Clim. Dyn.*, doi:10.1007/s00382-012-1575-x.

Patla, J. E., D. Stevens, and G. M. Barnes (2009), A conceptual model for the influence of TUTT cells on tropical cyclone motion in the northwest Pacific Ocean, *Weather Forecast.*, *24*, 1215–1235, doi:10.1175/2009WAF2222181.1.

Rinke, A., P. Marbaix, and K. Dethloff (2004), Internal variability in Arctic regional climate simulations: Case study for the SHEBA year, *Clim. Res.*, *27*, 197–209.

Sadler, J. C. (1976), A role of the tropical upper tropospheric trough in early season typhoon development, *Mon. Weather Rev.*, *104*, 1266–1278, doi:10.1175/1520-0493(1976)104<1266:AROTTU>2.0.CO;2.

Sadler, J. C. (1978), Mid-season typhoon development and intensity changes and the tropical upper tropospheric trough, *Mon. Weather Rev.*, *106*, 1137–1152, doi:10.1175/1520-0493(1978)106<1137:MSTDAI>2.0.CO;2.

Shutts, G. J. (2005), A kinetic energy backscatter algorithm for use in ensemble prediction systems, *Q. J. R. Meteorol. Soc.*, *131*, 3079–3102, doi:10.1256/qj.04.106.

Shutts, G. J., and T. N. Palmer (2007), Convective forcing fluctuations in a cloud-resolving model: Relevance to the stochastic parameterization problem, *J. Clim.*, *20*, 187–202, doi:10.1175/JCLI3954.1.

Simmons, A., S. Uppala, D. Dee, and S. Kobayashi (2006), ERA-Interim: New ECMWF reanalysis products from 1989 onwards. ECMWF Newsletter, No. 110, 26–35, ECMWF, Reading, U. K.

Skamarock, W., J. Klemp, J. Dudhia, D. Gill, D. Barker, W. Wang, and J. Powers (2008), A description of the advanced research WRF version 3, *NCAR Tech. Note 475*.

Suzuki-Parker, A. (2012), An assessment of uncertainties and limitations in simulating tropical cyclones, Springer thesis, XIII, 78 pp.

Thorncroft, C., and K. Hodges (2001), African easterly wave variability and its relationship to Atlantic tropical cyclone activity, *J. Clim.*, *14*, 1166–1179, doi:10.1175/1520-0442(2001)0142.0.CO;2.

Vannitsem, S., and F. Chomé (2005), One-way nested regional climate simulations and domain size, *J. Clim.*, *18*, 229–233, doi:10.1175/JCLI3252.1.

Vecchi, G. A., and G. Villarini (2014), Next season's hurricanes, *Science*, *343*, 618–619, doi:10.1126/science.1247759.

Villarini, G., and G. A. Vecchi (2012), Twenty-first-century projections of North Atlantic tropical storms from CMIP5 models, *Nat. Clim. Change*, *2*, 604–607, doi:10.1038/nclimate1530.

Wu, C.-C., R. Zhan, and Y. Wang (2012), Internal variability of the dynamically downscaled tropical cyclone activity over the western North Pacific by the IPRC Regional Climate Model, *J. Clim.*, *25*, 2104–2122, doi:10.1175/JCLI-D-11-00143.1.

Zhang, F., and D. Tao (2013), Effects of vertical wind shear on the predictability of tropical cyclones, *J. Atmos. Sci.*, *70*, 975–983, doi:10.1175/JAS-D-12-0133.1.

Zhao, M., I. M. Held, S. J. Lin, and G. A. Vecchi (2009), Simulations of global hurricane climatology, interannual variability, and response to global warming using a 50 km resolution GCM, *J. Clim.*, *22*, 6653–6678, doi:10.1175/2009JCLI3049.1.